

NASA  
TP  
1275  
c.1

## NASA Technical Paper 1275

LOAN COPY: RETURN  
AFWL TECHNICAL LIBRARY  
KIRTLAND AFB, N.M.

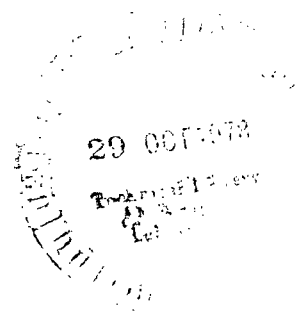


# Quantitative Mapping by Remote Sensing of an Ocean Acid-Waste Dump

Craig W. Ohlhorst

OCTOBER 1978

**NASA**





NASA Technical Paper 1275

# Quantitative Mapping by Remote Sensing of an Ocean Acid-Waste Dump

Craig W. Ohlhorst  
*Langley Research Center  
Hampton, Virginia*



National Aeronautics  
and Space Administration

**Scientific and Technical  
Information Office**

1978



## CONTENTS

SUMMARY . . . . .	1
INTRODUCTION . . . . .	1
EXPERIMENT . . . . .	2
DATA ANALYSIS, RESULTS, AND DISCUSSION . . . . .	3
In Situ Water Sample Analysis . . . . .	3
Quantitative Analysis . . . . .	3
Particulate iron . . . . .	5
Suspended solids . . . . .	7
CONCLUDING REMARKS . . . . .	7
APPENDIX - CLASSIFICATION TECHNIQUE . . . . .	9
REFERENCES . . . . .	11
TABLES . . . . .	12
FIGURES . . . . .	16

## SUMMARY

A remote sensing experiment was conducted at an ocean acid-waste dump site off the coast of Delaware. Results are presented which show that a multispectral scanner on an airplane platform flown at an altitude of 914 m can be used to quantify and map an acid-waste dump in terms of its particulate iron concentration. The same data, however, could not be used to map the dump in terms of total suspended solids, organic suspended solids, or inorganic suspended solids concentrations. A two-step approach was used to map the acid-waste dump. The first step was to apply a classification technique to differentiate between spectral signature changes to the background ocean water caused by the acid and those caused by Sun glitter. The second step was to quantify the iron concentration in the acid-waste dump by use of a single-variable equation using the ratio of band 2 (440 to 490 nm) radiance to band 4 (540 to 580 nm) radiance. Particulate iron concentrations in the acid waste were found to range up to 1.1 mg/l at a depth of 0.46 m. The acid-waste dump which was quantitatively mapped varied in age from freshly dumped to  $3\frac{1}{2}$  hr.

## INTRODUCTION

The oceans have been used as a disposal site for vast quantities of dredged material, municipal wastes, and industrial wastes for many years, with little known about the impact of this dumping on the ocean environment. In 1972, the National Oceanic and Atmospheric Administration (NOAA), in coordination with the U.S. Coast Guard (USCG), and the Environmental Protection Agency (EPA) were assigned the responsibility under the Marine Protection, Research, and Sanctuaries Act of establishing a comprehensive program of monitoring and research to determine the effects of ocean dumped materials on the marine environment (ref. 1). Both NOAA and EPA have requested that the National Aeronautics and Space Administration (NASA) join with them in cooperative programs to assess the role of remote sensing in meeting their monitoring and research needs.

Two of the major ocean dumped materials are municipal sewage sludge and industrial acid waste. Both of these have been detected by aircraft and satellite remote sensors (refs. 2 to 5). Quantification and mapping of suspended solids in municipal sewage sludge dumps have been demonstrated by use of airplane remote sensing data (ref. 6). Little has been done, however, to quantify and map acid-waste dumps with the use of remote sensing data.

In order to assess the possibility of relating remotely sensed spectral signatures to acid-waste concentrations, the NASA Langley Research Center, in conjunction with the University of Delaware, conducted an experiment at an ocean acid-waste dump site off the coast of Delaware on August 28, 1975. In situ water samples and measurements, along with concurrent remotely sensed data, were obtained at the dump site. This paper summarizes the results of

the analyses for quantifying and mapping the acid-waste plume in terms of its particulate iron concentration and its suspended solids concentration.

## EXPERIMENT

The acid waste in this experiment was the waste product from a titanium dioxide processing plant at Edgemoor, Delaware. The waste was a hydrochloric acid solution containing a number of metal impurities, among which iron was the major one. When the waste was dumped into the ocean, the hydrochloric acid was neutralized and the iron reacted with the ocean water to produce a ferric hydroxide precipitate. The acid-waste disposal site was located approximately 70 km southeast of Cape May, New Jersey. (See fig. 1.) The site was a 9.3 by 14.8 km rectangular area bounded by  $38^{\circ}30'$  and  $38^{\circ}35'$  north latitudes and by  $74^{\circ}15'$  and  $74^{\circ}25'$  west longitudes. The waste was carried to the site by barge, then dumped while the barge traveled in a bow-tie pattern at a speed of around 8 knots; approximately 1 million gallons of waste were dumped in about 4 hr.

The experiment was performed on August 28, 1975. The barge started dumping at 0650 EDT and finished dumping around 1100 EDT. In situ water samples were collected by ship at 10 locations between the hours of 0944 EDT and 1326 EDT, with sampling stations selected to obtain a wide variation in plume age. Nine of these stations were located in the acid plume, with the tenth station being located outside the plume as a control. (See fig. 2.) At seven of the stations, water samples were taken at depths of 0.46, 4, and 8 m with 5-l Niskin bottles; Secchi disc depth and pH measurements were made at these stations. At the other three sample stations, only bucket surface samples were taken. Measurements of pH were made on these surface samples, but Secchi disc depths were not measured. The station numbers (indicated in fig. 2), time of sampling, Sun elevation and azimuth angles, plume age, Secchi disc depth, sampling depth, suspended solids concentrations, and particulate iron concentrations are listed in table I.

The multispectral scanner was flown over the dump site in a twin-engine airplane at an altitude of 914 m. Flight lines were flown such that spectral radiance data were collected concurrently with in situ water sampling at nine of the stations and 35 min after sampling for station 4-2. The multispectral scanner is an 11-band instrument, with 10 bands in the visible and near infrared and one in the thermal band range. The spectral and spatial characteristics of the instrument are given in table II.

The radiance data were obtained in the form of nine-track 800-bpi computer compatible tapes. Screening imagery (film-reader product) of band 5 (580 to 620 nm) was also obtained and aided in determining areas of interest. Use of in-flight calibration data converted the digital counts to radiance values ( $\text{mW}/\text{cm}^2\text{-sr-band}$ ). The high noise level in band 1 (380 to 440 nm) precluded the use of that band for data analysis. At the 914-m altitude, the level of radiance recorded in band 10 (970 to 1060 nm) was essentially zero; consequently, that band was omitted from the analysis. More detailed discussions of this experiment are given in references 7 and 8.

## DATA ANALYSIS, RESULTS, AND DISCUSSION

### In Situ Water Sample Analysis

Sampling times and location of data stations were such that the age of the sampled plume sections ranged between  $1\frac{1}{2}$  hr and 4 hr. The particulate iron concentration ranged from 0.21 to 2.32 mg/l in the plume. Total suspended solids ranged from 2.1 to 15.1 mg/l, inorganic suspended solids were measured up to 5.6 mg/l, and organic suspended solids were measured up to 9.5 mg/l in the acid plume. For the control station 1-2, the particulate iron concentration was less than 0.05 mg/l at all three depths, and the total suspended solids concentration ranged from 1.1 to 8.1 mg/l.

A decreasing concentration with increasing depth was evident for both particulate iron and suspended solids in the plume between the bucket surface samples and the 0.46-m depth samples. Because of the magnitude of the concentration difference between the surface and 0.46-m depth samples, it was decided that the three bucket surface sample stations (stations 2-2, 2-3, and 4-3) should be left out of the analysis. With this deletion, the number of in situ sample stations was reduced to seven (six in the plume and one control).

The average Secchi disc depth measurement in the plume was 3 m. At the control station, the Secchi disc depth was 4.25 m. Little, if any, radiance received by the remote sensor is thought to originate from water depths below the Secchi disc depth; therefore, correlation between the 4- and 8-m depth sample concentrations and scanner radiance values was thought to be poor. Subsequent regression analysis proved that assumption to be correct. Only the regression-analysis results between the remotely sensed radiance data and the 0.46-m depth concentrations are discussed here.

### Quantitative Analysis

For all sampling stations except station 4-2, the boat's position was located in the remotely sensed data. The boat location of station 4-4 was used to approximate the location of station 4-2 in the remotely sensed data. Each station was located at or near the nadir position in the scanner data. For all sampling stations, an adjacent 3-by-4 pixel area was chosen as representative of the spectral signature for that station. The 3-by-4 pixel area was used to approximate a square footprint. Subsequent analysis showed a 3-by-4 pixel area to be sufficient to average out spectral and spatial noise errors. At 914 m, the instantaneous pixel size was a surface 2.3 m on a side.

Quantitative mapping of the acid waste was attempted in terms of both the particulate iron concentration and the suspended solids concentration. The particulate iron concentration was chosen as a parameter because laboratory results (Lewis and Collins, ref. 8) have shown that the amount of particulate iron has a major influence on the spectral signature of the acid waste. Because total suspended solids concentration has been found to correlate well with spectral data from a sewage sludge ocean dump (ref. 6), it was also considered.

For the analysis, a linear relationship was used between the measured radiance values (or radiance functions) and the in situ parameter concentration. Under this condition,

$$C = a_0 + \sum_{i=1}^n a_i R_i' + e \quad (1)$$

where  $R_i'$  are radiance functions, defined as the original single band radiance values  $R$  or any radiance parameter values that are derived from the transformation techniques used to reduce the effect of Sun elevation angle. In equation (1),  $C$  is concentration of the in situ parameter,  $a_0, a_i, \dots, a_n$  are coefficients, and  $e$  is error.

Factors that could affect the absolute magnitude of the individual band radiance values are discussed in the following paragraphs.

Instrument noise: Instrument noise was reduced in the set of radiance values corresponding to the seven data stations by averaging a 3-by-4 pixel area.

Atmospheric backscatter: Analysis of radiance data collected from nadir to  $\pm 40^\circ$  over background ocean water showed no appreciable change in the magnitude of the radiance levels; therefore, it was assumed that there was no atmospheric effect from increases in atmospheric path length due to scan angle.

Sun elevation angle: The Sun elevation angle varied between  $39^\circ$  and  $62^\circ$  (see table I) during the time span of the experiment. The original unadjusted radiance values assigned to the seven stations (six plumes and one control) and background-water values in the vicinity of each plume station are presented in table III. These radiance values show a general trend of increasing magnitude with increasing Sun angle. For the purpose of reducing the effect of Sun angle changes on the radiance data and thus the degree of error attributed to this factor, a number of data transformations were performed on the original unadjusted radiance values. The following techniques were tested on the radiance values:

(1) All possible ratios between individual band radiance values were calculated.

(2) At each station, the radiance values in each band were divided by the sum total radiance of the eight bands. The number assigned to each band was thus the percentage of the total radiance contributed by that band.

(3) The background-water radiance values in the vicinity of each plume station were subtracted from the plume-station radiance values. For the control station 1-2, the resultant radiance value was zero for each band.

(4) At each station, the radiance values were divided by the cosine of the Sun zenith angle.



Sun glitter: Sun glitter is the direct specular reflection of the incident light off the water surface into the sensor. Sun glitter was encountered during some of the overflights, and it caused the radiance levels measured at the remote sensor to be higher than normally expected for background ocean water areas. From examination of the radiance data, the acid-plume areas also had higher radiance levels than the surrounding background water. The first step leading to an accurate quantification was to differentiate between high-radiance-level spectral signatures caused by the acid and those resulting from Sun glitter. A classification technique was derived to separate these signatures. A short discussion of the technique is given in the appendix, and the derivation of it is described by Gilbert S. Bahn in reference 9. Figure 3 shows a black and white image of band 4 radiance for the remotely sensed data collected during the sensor overpass of the control station 1-2. The delineating radiance value ( $0.106 \text{ mW/cm}^2\text{-sr-band}$ ) was somewhat arbitrary. The chosen value was subjectively preferable in pictorial terms to help demonstrate use of the classification technique. The acid waste with its higher radiance level is white, while most of the background water is black. The right-hand third of the photograph is predominately white in color, which might inherently imply that the area was part of the acid plume. The classification scheme identified most of the pixels in the right-hand third of the photograph to be affected by Sun glitter. (See fig. 4(a).) In figure 4(b), the acid waste is white, while the Sun-glitter and background-water classes are shown in black.

Linear regression analysis, stepwise regression analysis, and multiple regression analysis techniques were examined in attempts to relate the spectral signatures to the iron and suspended solids concentrations. Regression analysis was first performed using the original unadjusted scanner radiance data. The transformed radiance data calculated from each of the transformation techniques discussed previously were subsequently examined.

Particulate iron.- The analysis indicated there was a strong relationship between the spectral signatures and iron concentrations. Quantitative mapping of the plume and surrounding background water was obtained from each of the equations derived in the analysis. An examination of correlation coefficients and subjective analysis of pictorial displays of the various quantitative mappings led to the choice of a single-variable equation that used a band ratio as the independent variable. The ratio chosen was that of band 2 (440 to 490 nm) radiance to band 4 (540 to 580 nm) radiance. The correlation coefficients between particulate iron and all possible band ratios are presented in table IV. Although a number of ratios had high correlations with iron, subjective analysis of pictorial quantitative mappings led to the choice of the band 2 to band 4 ratio. The equation developed for iron concentration, in  $\text{mg/l}$ , was

$$\text{Iron} = 2.22 - 1.05(R_2/R_4) \quad (2)$$

where  $R_2$  and  $R_4$  are the original unadjusted radiances of band 2 and band 4, respectively. A plot of particulate iron concentration as a function of the ratio is shown in figure 5. The dotted line represents the linear least-squares equation that fits the data. (See eq. (2).) The correlation coeffi-

cient between the ratio and the particulate iron concentration was -0.95. The standard error of estimate was 0.1 mg/l, and the value of the F-ratio was 45.4.

Three sections of the plume ranging in age from freshly dumped to  $3\frac{1}{2}$  hr were selected for quantification mapping of iron concentration. Two of these plume sections were covered by the flight line over the control station 1-2. The corresponding spectral data were first passed through the classification algorithm and then were quantitatively mapped according to equation (2) on a pixel by pixel basis. Any pixel that was classified as a Sun-glitter pixel was assigned a concentration of zero. Figure 6 shows the resultant quantification map for plume pixels. Calculated iron concentrations in excess of 0.25 mg/l are shown. The square box seen in the photograph encloses the dumping barge. The section of acid-waste plume trailing behind the barge is approximately 20 min old at the right-hand edge of figure 6. The acid waste goes through a series of chemical reactions after contact with the ocean water, and iron hydroxide precipitates out. A mixing zone can be picked out immediately behind the barge. This is an area of low iron concentration calculated to be from 0.45 to 0.75 mg/l. More complete mixing of the waste is indicated by the sudden increase in calculated iron concentration up to 1.10 mg/l. Behind the mixing zone, the iron concentrations are calculated to be fairly constant, with concentrations ranging from 1.10 mg/l at the center to about 0.75 mg/l at the edges. The width of this fresh section is approximately 50 m.

The plume shown on the left side of figure 6 has been in the water on the average of  $3\frac{1}{2}$  hr. The highest concentrations of the center are now calculated to be 0.65 mg/l. Concentrations decrease to 0.25 mg/l at the edges. These lower concentrations would be expected since the iron hydroxide has had time to settle and the plume has been dispersed. The wind was from the northeast on the day of the experiment, and this plume section has undergone considerable dispersion downwind. The acid waste has undergone less dispersion perpendicular to the wind direction, as indicated by the many sharp projections that are still differentiable. In the direction of the wind, certain areas of the plume have spread out to about 250 m wide.

The third section of the plume that has been quantitatively mapped is shown in figure 7. The acid had been in the water approximately  $1\frac{1}{3}$  hr when the remotely sensed data were collected. The calculated iron concentration in the center of the plume in the lower right-hand corner is between 0.95 and 1.10 mg/l. In other parts of this photograph, the center concentration is calculated to be somewhat lower (between 0.65 and 0.85 mg/l). As the plume dispersed, the iron concentrations decreased to about 0.45 mg/l at the plume edges.

The spectral data in figure 7 were taken simultaneously with sample collection at station 3-1. The calculated iron concentration at this station was 0.77 mg/l and the measured concentration was 0.78 mg/l. The wind direction was

still from the northeast when the spectral data were taken. The quantification map is consistent in that the width of the 0.45 mg/l plume edge is more extensive in the northeast direction. In the upper portion of figure 7, the plume has dispersed to about 190-m width, which is less than the 250-m width for the

$\frac{1}{2}$  3-hr old section shown in figure 6.

The sample taken at the control station 1-2 had a laboratory measured particulate iron concentration of 0.05 mg/l. Fifty percent of the background-water area in both figures 6 and 7 unaffected by Sun glitter was calculated to have zero iron concentration and ninety percent was calculated to have less than 0.25 mg/l of iron hydroxide. The higher concentrations of the other 10 percent was attributed to instrument noise.

Suspended solids.- Quantification and mapping of the acid waste was also attempted using the suspended solids data. The concentration of total suspended solids and its two components (organic suspended solids and inorganic suspended solids) were all individually correlated to the remotely sensed radiance data. The best correlations were calculated with the use of the radiance-data transformation technique discussed previously whereby the clear-water radiance values were subtracted from the plume radiance values. The resultant linear least-squares equations for suspended solids, in mg/l, were as follows:

$$\text{Total suspended solids} = 3.09 + 153.91R_8' \quad (r = 0.824) \quad (3)$$

$$\text{Organic suspended solids} = 1.33 + 111.76R_8' \quad (r = 0.872) \quad (4)$$

$$\text{Inorganic suspended solids} = 1.56 + 0.01R_4' \quad (r = 0.716) \quad (5)$$

where  $R_4'$  and  $R_8'$  are the plume values minus clear-water radiance values for band 4 and band 8, respectively. Equations (3) to (5) were applied to the same two scenes of radiance data as was the iron equation. Pictorial displays of the calculated concentration maps of all three suspended solids parameters were such that the plume could not be distinguished from the surrounding water. One of the reasons for the lack of separation was that the concentration of suspended material at the control station was higher at the 0.46-m depth than that at two of the plume stations. It was concluded that in this data set the acid-waste plume could not be accurately quantified and mapped in terms of total suspended solids, organic suspended solids, or inorganic suspended solids.

The ability to quantify and map the ocean acid dump in terms of particulate iron concentration, but not with total suspended solids parameters, is in agreement with laboratory studies (ref. 8) that have indicated the concentration of particulate iron in the form of iron hydroxide to be the major factor which dictates the spectral signature of the acid waste in the ocean.

#### CONCLUDING REMARKS

Results from this analysis show that airplane remotely sensed spectral data can be used to quantify and map an acid-waste dump. A relationship has been

found between the remotely sensed spectral signatures and the particulate iron concentrations in the acid waste. This relationship has led to the quantification and mapping of the acid dump in terms of the iron concentration. A linear least-squares-fit equation employing the ratio of band 2 (440 to 490 nm) radiance to band 4 (540 to 580 nm) radiance was used to calculate iron concentration. Particulate iron concentrations in the plume were found to range up to 1.1 mg/l at a depth of 0.46 m.

A classification technique was developed to identify Sun-glitter affected pixels in the background-water data. Application of this technique leads to more accurate quantitative mapping.

Langley Research Center  
National Aeronautics and Space Administration  
Hampton, VA 23665  
August 24, 1978

## APPENDIX

### CLASSIFICATION TECHNIQUE

A classification technique used to identify Sun-glitter pixels is presented in this appendix.

Initial analysis had shown that the ratio of band 2 radiance ( $R_2$ ) to band 4 radiance ( $R_4$ ) would discriminate the acid waste from the normal background ocean water, but  $R_2/R_4$  was not always adequate to separate the waste from background areas affected by Sun glitter. Various parameters were tried in order to sort pixels into three different classes (acid waste, Sun glitter, and normal background water). Eventually, two parameters evolved that could be used to separate the acid waste from the Sun-glitter affected pixels when used in conjunction with the original band 4 radiance ( $R_4$ ).

The first parameter  $X_1$  was a function of the adjusted radiance values  $R_3^*$ ,  $R_4^*$ , and  $R_5^*$  in band 3, band 4, and band 5, respectively. The second parameter  $X_2$  was a function of the adjusted radiance values  $R_6^*$ ,  $R_7^*$ , and  $R_8^*$  in band 6, band 7, and band 8, respectively. The adjusted radiance values are defined in step 4 of the classification scheme discussed below. The two parameters were as follows:

$$X_1 = 1.7947R_3^* + 2.4857R_4^* + 2.1276R_5^* - 16.104$$

$$X_2 = 2.5391R_6^* + 3.1290R_7^* + 5.2304R_8^* - 6.536$$

Use of three bands in each parameter tended to minimize noise levels. Both parameters are nominal measures of the influence of the acid waste in elevating the background-water spectral signature level. For values of  $X_1$  less than or equal to zero, the pixel was simply classified as either a background-water pixel or a Sun-glitter affected pixel, depending on the value of  $R_4$ . A function  $Y(X_1)$  was empirically derived to distinguish a boundary between acid-waste pixels and all other pixels when  $X_1$  exceeded zero. The equation of the boundary function for  $X_1 < 10.3$  was

$$Y = -0.009 + 0.2303X_1 + 0.0310X_1^2 - 0.00123X_1^3 + 0.0004015X_1^4$$

and for  $X_1 \geq 10.3$  was

$$Y = 2.8X_1 - 20$$

The boundary function  $Y$  and the distinguishing value of  $R_4$  were developed subjectively by making trial calculations and pictorially displaying the results as false-color images on a television screen. Because of noise in the recorded data,  $Y$  and  $R_4$  are approximations for the definitive criteria desired. The boundary values for the classification technique are presented in table AI.

## APPENDIX

TABLE AI.- BOUNDARY VALUES FOR CLASSIFICATION SCHEME

Pixel	Boundary values
Background water	$X_1 \leq 0$ or $X_2 - X_1 \geq Y$ ; $R_4 < 0.118 \text{ mW/cm}^2\text{-sr-band}$
Sun glitter	$X_1 \leq 0$ or $X_2 - X_1 \geq Y$ ; $R_4 \geq 0.118 \text{ mW/cm}^2\text{-sr-band}$
Acid waste	$X_1 > 0$ or $X_2 - X_1 < Y$

The classification scheme proceeded in six steps as follows:

(1) Initially,  $X_1$  and  $X_2$  were computed from the original radiance data for each pixel.

(2) Classification was performed according to the parameter limits shown in table AI in order to identify acid-waste pixels.

(3) Vertical column average radiance values were computed for each radiance band using only those pixels not assigned to the acid-waste category.<sup>a</sup> The minimum average value in each band was assigned to be the base value for that band.

(4) All of the original radiance data were then adjusted by subtracting the column average background radiance from the individual pixel radiance in that column and adding the difference to the assigned base value.

(5) Again,  $X_1$  and  $X_2$  were calculated using the adjusted radiances.

(6) Classification was performed according to the parameter limits shown in table AI in order to identify plume pixels.

Except for keeping the assigned base values constant, steps 3 through 6 were repeated as many times as required until there was no practical change in the total number of acid-waste classified pixels. It was found that two iterations were sufficient to classify the pixels in the data shown in figure 4 while three iterations were used on the data shown in figure 7. Although the coefficients of  $X_1$ ,  $X_2$ , and  $Y$  relate specifically to this experiment, the general form of these equations may have wider application.

---

<sup>a</sup>As iteration proceeded, the column averages were always calculated with the original unadjusted radiance values.

## REFERENCES

1. Report to the Congress on Ocean Dumping Research - January through December 1975. NOAA, U.S. Dep. Commer., June 1976.
2. Wezernak, C. T.; and Roller, N.: Monitoring Ocean Dumping With ERTS-1 Data. Symposium on Significant Results Obtained From the Earth Resources Technology Satellite-1, Volume I: Technical Presentations - Section A, NASA SP-327, 1973, pp. 635-641.
3. Mairs, Robert L.; Wobber, Frank J.; Garofalo, Donald; and Yunghans, Roland: Application of ERTS-1 Data to the Protection and Management of New Jersey's Coastal Environment. Symposium on Significant Results Obtained From the Earth Resources Technology Satellite-1, Volume I: Technical Presentations - Section A, NASA SP-327, 1973, pp. 629-634.
4. Wezernak, C. T.; Lyzenga, D. R.; and Polcyn, F. C.: Remote Sensing Studies in the New York Bight. Rep. No. 109300-5-F (NOAA Grant No. 04-4-158-33), Environ. Res. Inst. of Michigan, July 1975.
5. Klemas, Vytautas; Bartlett, David S.; Philpot, William D.; Rogers, Robert H.; and Reed, Larry E.: Skylab/EREP Application to Ecological, Geological, and Oceanographic Investigations of Delaware Bay. CMS-NASA-1-76 (NAS1-12304), Univ. of Delaware, May 1976.
6. Johnson, R. W.; Duedall, I. W.; Glasgow, R. M.; Proni, J. R.; and Nelsen, T. A.: Quantitative Mapping of Suspended Solids in Wastewater Sludge Plumes in the New York Bight Apex. J. Water Pollut. Control Fed., vol. 49, no. 10, Oct. 1977, pp. 2063-2073.
7. Hypes, Warren D.; and Ohlhorst, Craig W.: A Summary of the Test Procedures and Operational Details of a Delaware River and an Ocean Dumping Pollution Monitoring Experiment Conducted August 28, 1975. NASA TM X-74005, 1977.
8. Lewis, Beverley W.; and Collins, Vernon G.: Remotely Sensed and Laboratory Spectral Signature Studies of an Ocean Dumped Acid Waste. NASA TN D-8467, 1977.
9. Bahn, Gilbert S.: Segregation of Acid Plume Pixels From Background Water Pixels, Signatures of Background Water and Dispersed Acid Plumes, and Implications for Calculation of Iron Concentration in Dense Plumes. NASA CR-145372, 1978.

TABLE I.- IN SITU STATION DATA AND CHEMICAL ANALYSIS OF WATER SAMPLES

Station	Sampling time, EDT	Sun elevation angle, deg	Sun azimuth angle, deg	Plume age, hr:min	Secchi disc depth, m	Sample depth, m	Suspended solids			Particulate iron, mg/l
							Total, mg/l	Inorganic, mg/l	Organic, mg/l	
1-1B	0944	39	108	2:52	3.25	0.46	3.1	1.6	1.5	0.62
						4	4.0	1.9	2.1	.67
						8	----	---	---	.42
1-2	1000	43	112	----	4.25	0.46	3.7	2.1	1.6	≤0.05
						4	1.1	.8	.3	≤.05
						8	8.1	3.7	4.4	≤.05
2-1	1040	48	122	1:37	2.75	0.46	4.8	2.1	2.7	0.93
						4	2.8	1.6	1.2	.55
						8	----	---	---	.51
2-2	1045	50	125	1:46	----	0	15.1	5.6	9.5	1.96
2-3	1050	50	126	1:50	----	0	14.3	5.2	9.1	2.32
3-1	1100	52	127	1:46	3.00	0.46	5.6	2.3	3.3	0.78
						4	4.7	2.0	2.7	1.06
						8	5.6	2.3	3.3	.88
4-2	1237	62	167	3:10	2.25	0.46	3.2	1.9	1.3	0.77
						4	2.1	1.1	1.0	.64
						8	----	---	---	.32
4-3	1258	62	180	3:32	----	0	7.9	3.7	4.2	1.08
4-4	1305	62	182	3:34	3.00	0.46	7.4	3.4	4.0	1.08
						4	2.4	1.1	1.3	.32
						8	----	---	---	.21
4-5	1326	61	194	4:00	3.00	0.46	5.2	2.0	3.2	0.70
						4	3.8	1.9	1.9	.62
						8	4.8	2.6	2.2	.51



TABLE II.- SPATIAL AND SPECTRAL CHARACTERISTICS OF MULTISPECTRAL SCANNER

Spatial characteristics:

Instantaneous field of view = 2.5 mrad (equivalent to a footprint of 2.3 m on a side at 914 m altitude)

Total field of view = 120° (100° active scan plus 20° for roll compensation) perpendicular to flight path

Band	Spectral characteristics	
	Range, nm	Bandwidth, nm
1	380 to 440	60
2	440 to 490	50
3	495 to 535	40
4	540 to 580	40
5	580 to 620	40
6	620 to 660	40
7	660 to 700	40
8	700 to 740	40
9	760 to 860	100
10	970 to 1 060	90
Thermal	8 000 to 13 000	5000

TABLE III.- ORIGINAL UNADJUSTED BAND RADIANCES<sup>a</sup>

Station	Plume-station radiance values, mW/cm <sup>2</sup> -sr-band, for band -							
	2	3	4	5	6	7	8	9
1-1B	0.199	0.204	0.117	0.103	0.067	0.057	0.027	0.032
1-2 (control)	.231	.216	.117	.109	.082	.078	.052	.087
2-1	.206	.244	.173	.196	.141	.109	.043	.044
3-1	.234	.266	.170	.169	.108	.082	.039	.044
4-2	.313	.348	.231	.205	.133	.105	.045	.054
4-4	.326	.398	.284	.247	.171	.131	.059	.059
4-5	.283	.333	.211	.200	.133	.108	.059	.091
Station	Background-water radiance values in vicinity of each station for band -							
	2	3	4	5	6	7	8	9
1-1B	0.166	0.159	0.079	0.065	0.048	0.042	0.022	0.027
1-2 (control)	.231	.216	.117	.109	.082	.078	.052	.087
2-1	.182	.174	.092	.072	.054	.045	.025	.034
3-1	.202	.196	.104	.085	.059	.052	.029	.039
4-2	.282	.271	.155	.128	.090	.086	.042	.069
4-4	.252	.248	.137	.108	.081	.068	.038	.054
4-5	.235	.223	.122	.102	.074	.066	.042	.058

<sup>a</sup>Values are averages of 3-by-4 pixel sets.

TABLE IV.- CORRELATION COEFFICIENTS BETWEEN PARTICULATE IRON  
AND ALL POSSIBLE RADIANCE RATIOS<sup>a</sup>

Band used as numerator in ratio

Band used as denominator in ratio	2	3	4	5	6	7	8	9	
	2	0	0.925	0.930	0.776	0.664	0.478	-0.333	-0.727
	3	-.936	0	.911	.640	.456	.060	-.719	-.859
	4	-.949	-.926	0	.157	-.080	-.586	-.886	-.914
	5	-.856	-.712	-.115	0	-.441	-.837	-.913	-.924
	6	-.728	-.473	.129	.409	0	-.946	-.934	-.927
	7	-.483	-.020	.570	.796	.938	0	-.880	-.893
	8	.235	.593	.826	.885	.896	.832	0	-.852
	9	.613	.785	.880	.890	.878	.849	.845	0

<sup>a</sup>As an example, the correlation coefficients between particulate iron and the radiance ratio  $R_2/R_9$  is 0.613.

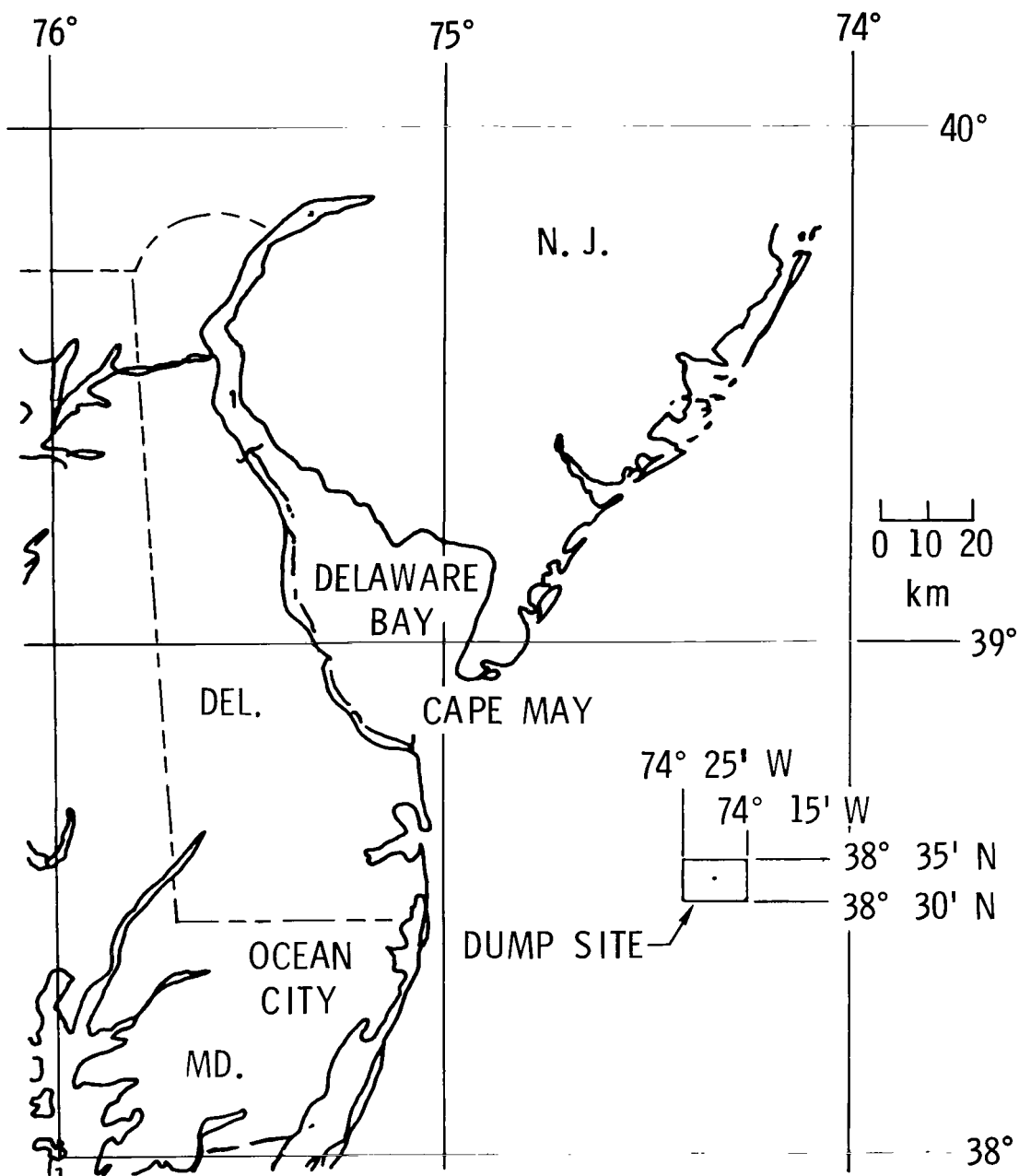


Figure 1.- Location of acid-waste dump site in Atlantic Ocean off coast of Delaware Bay.

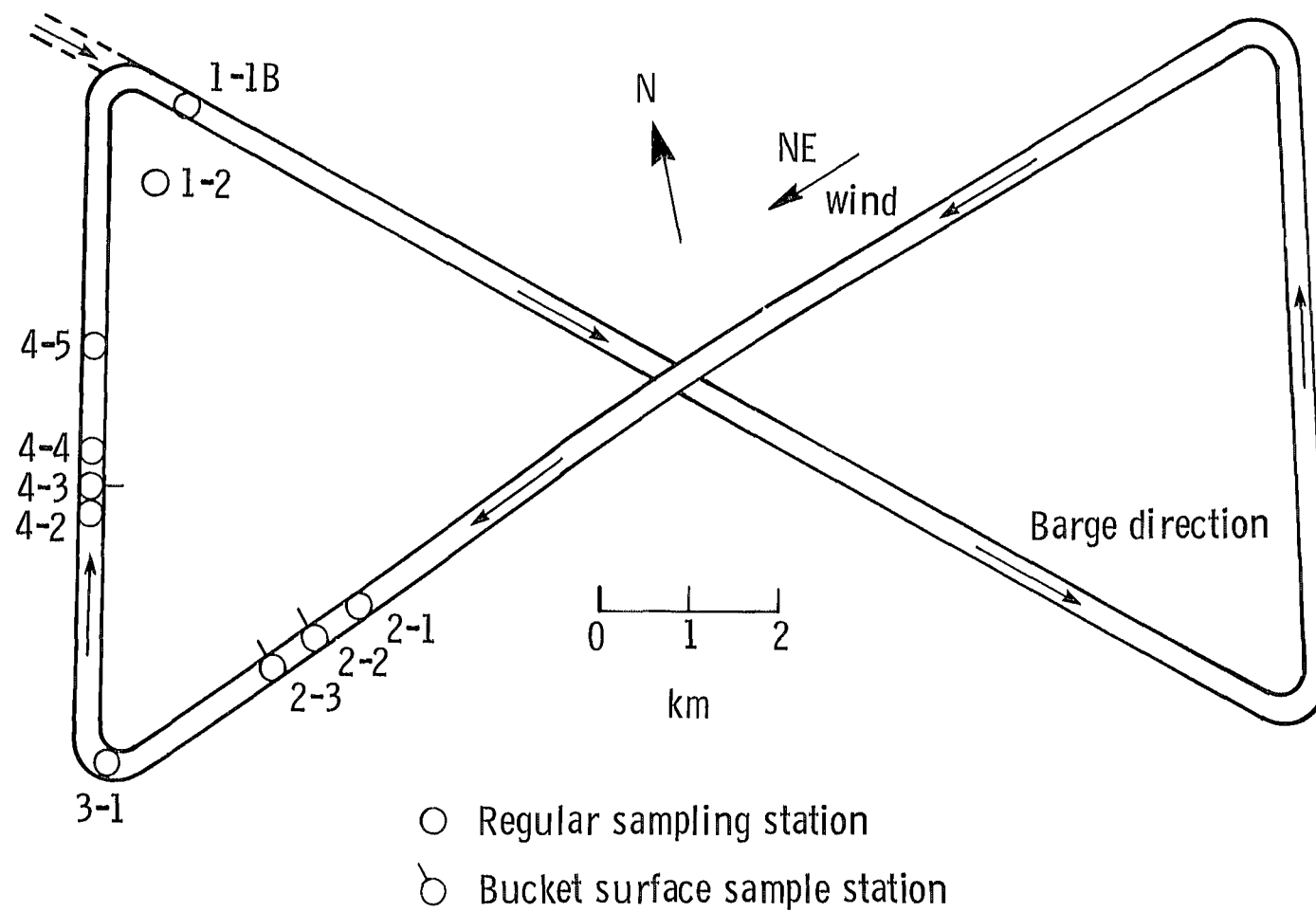
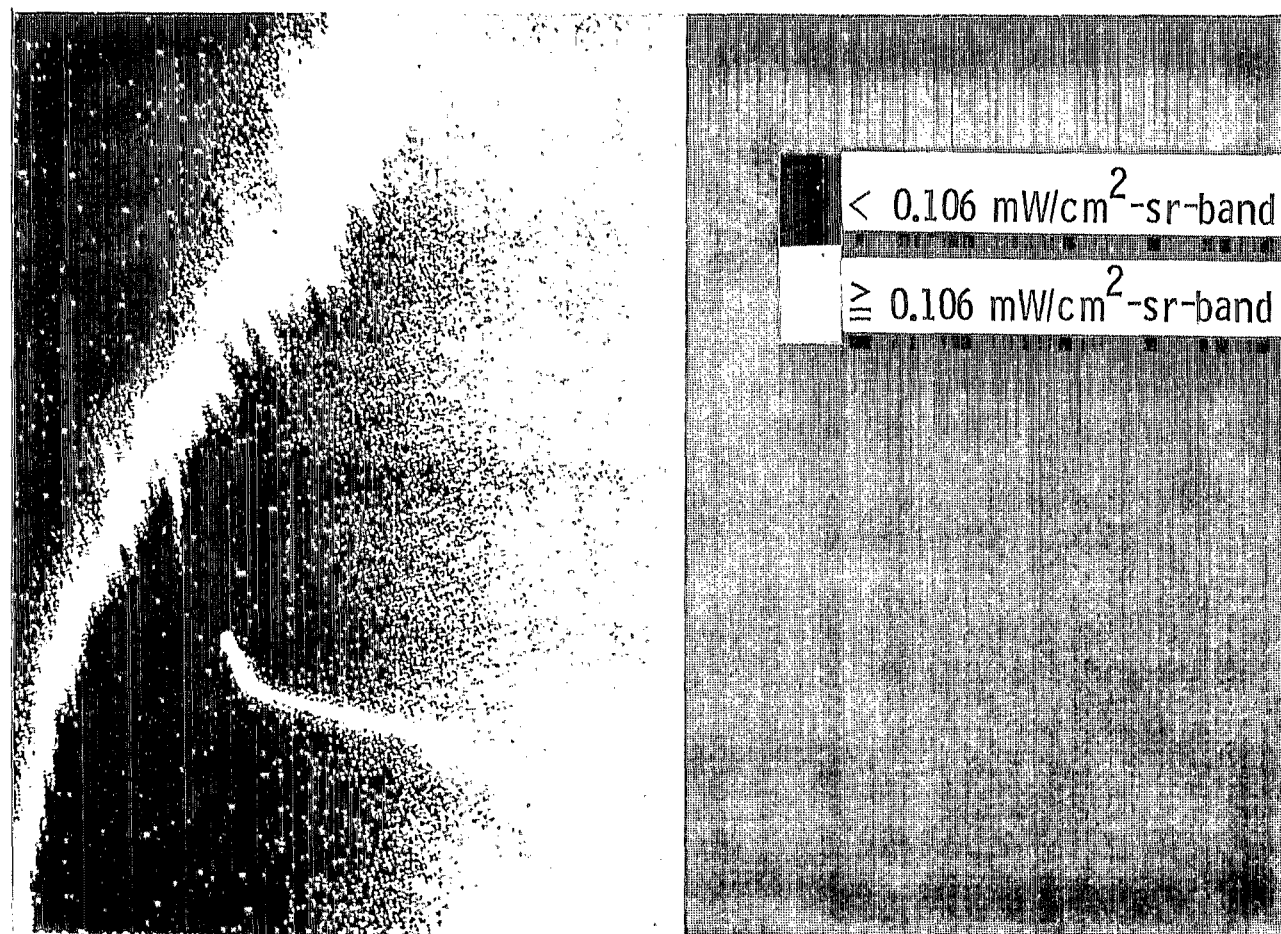
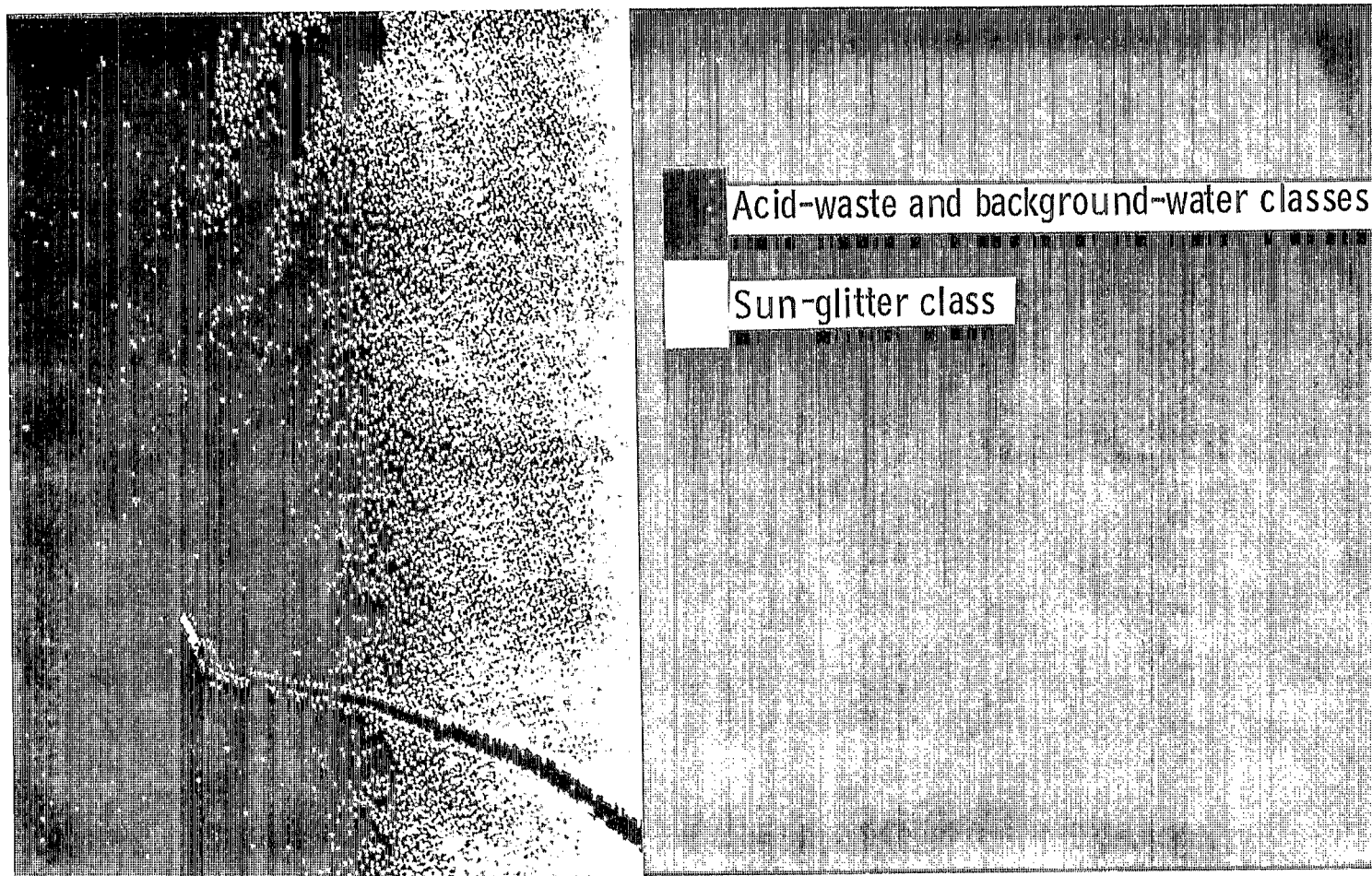


Figure 2.- Bow-tie path of dump barge, with positions of in situ sampling stations.



L-78-118

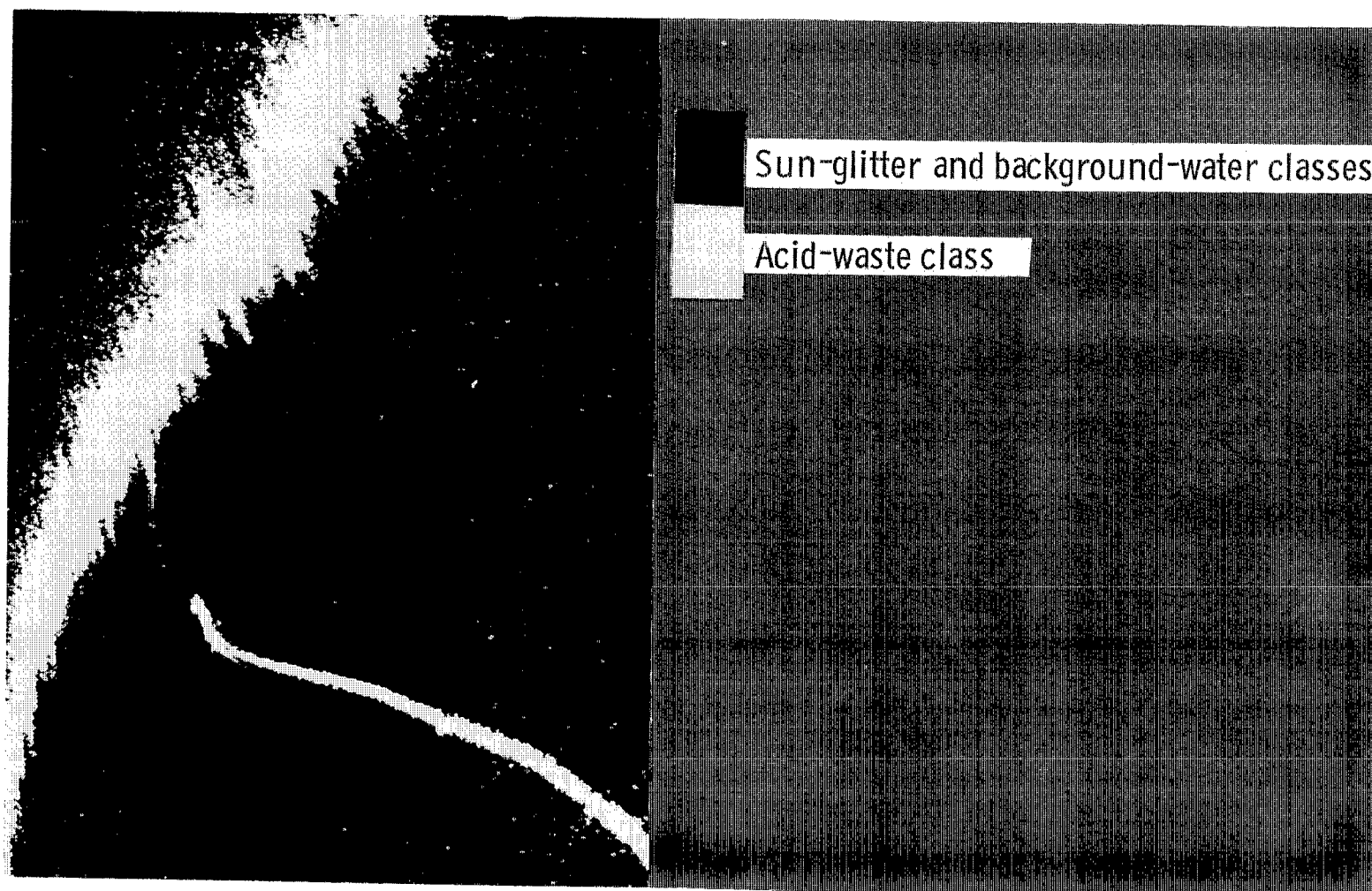
Figure 3.- Black and white presentation of band 4 radiance collected on flight line over station 1-2. (Data set consists of every line and every other column.)



L-78-119

(a) Separation of Sun-glitter class from data set.

Figure 4.- Illustration of classification technique to categorize spectral data collected on flight line over station 1-2. (Data set consists of every line and every other column.)



L-78-120

(b) Separation of acid-waste class from data set.

Figure 4.- Concluded.



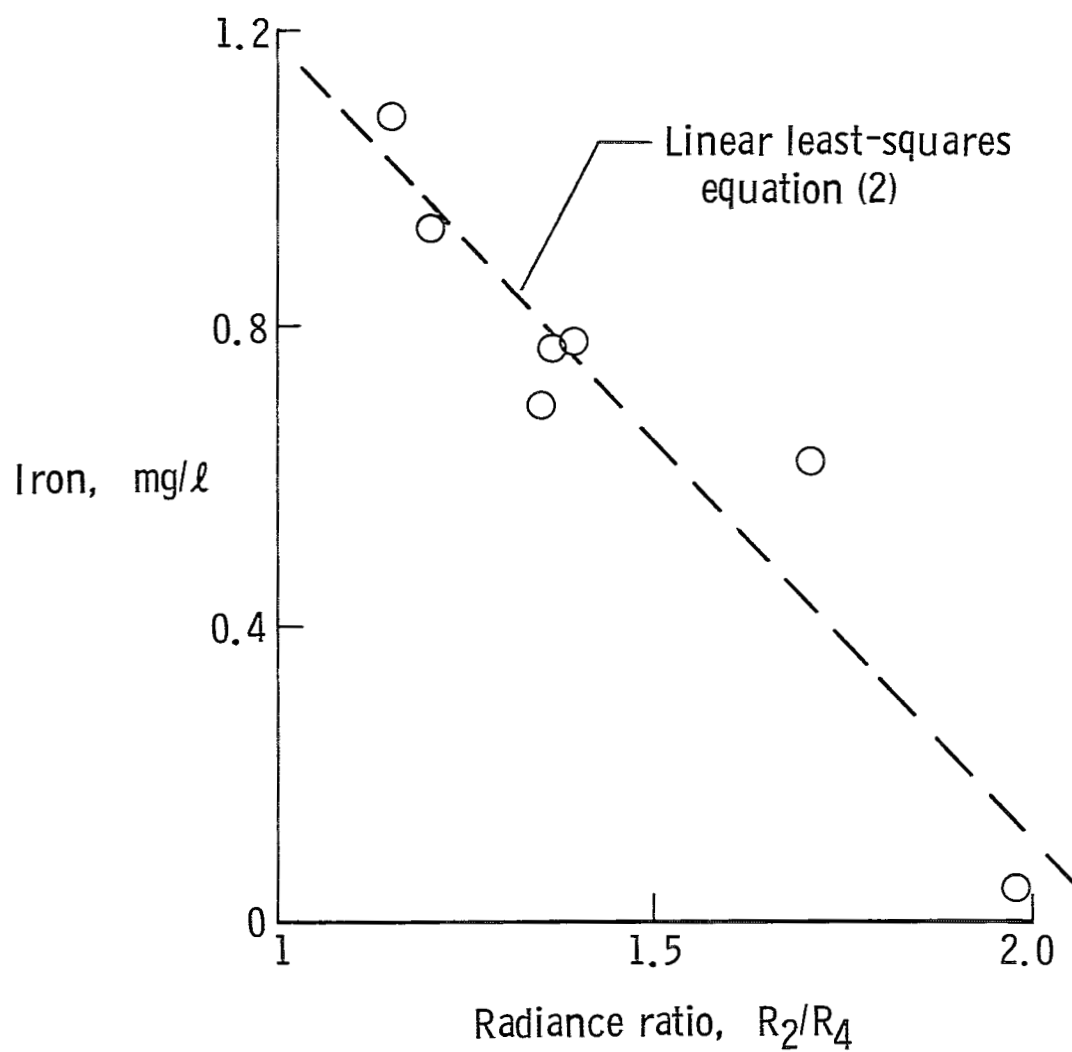
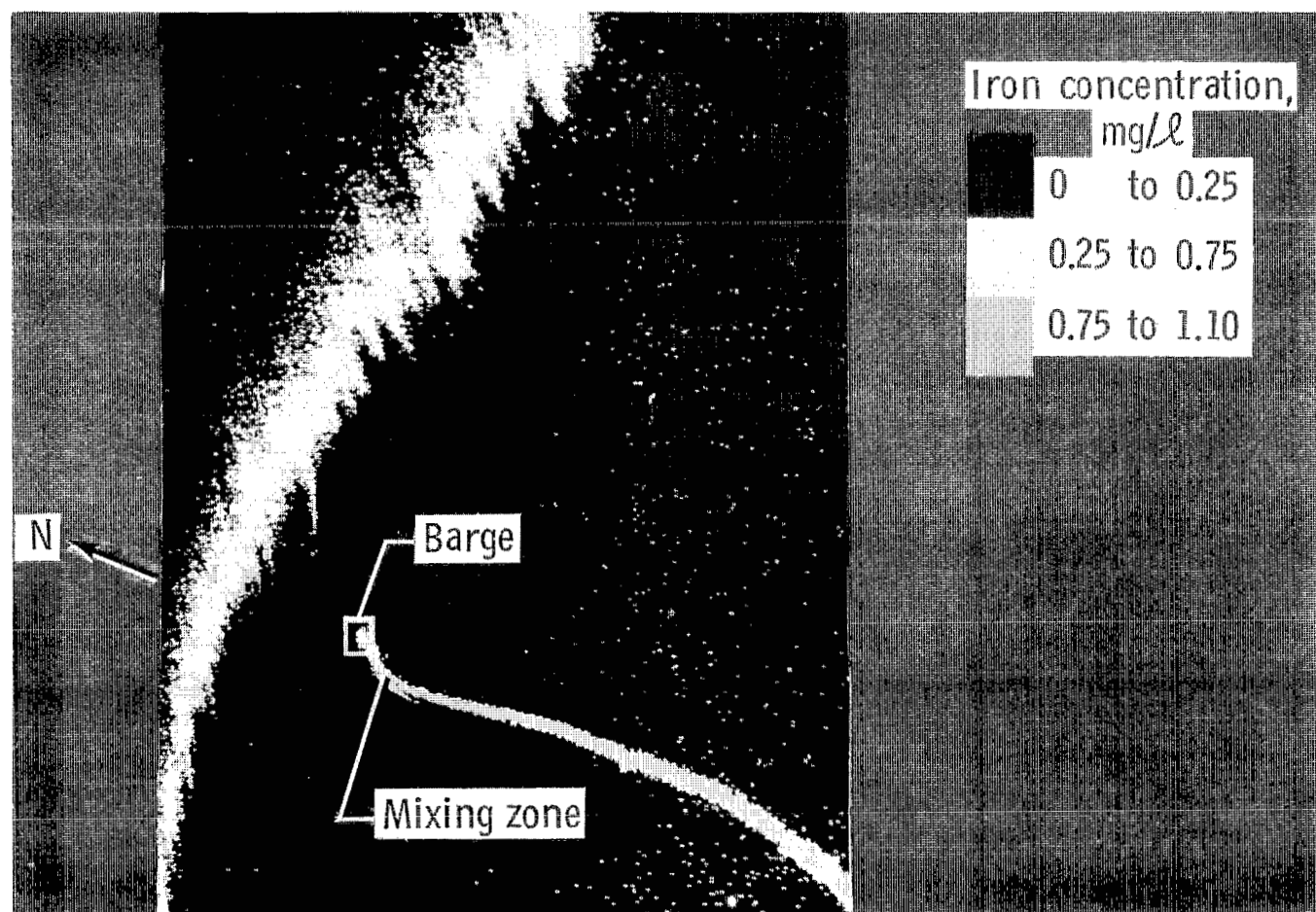
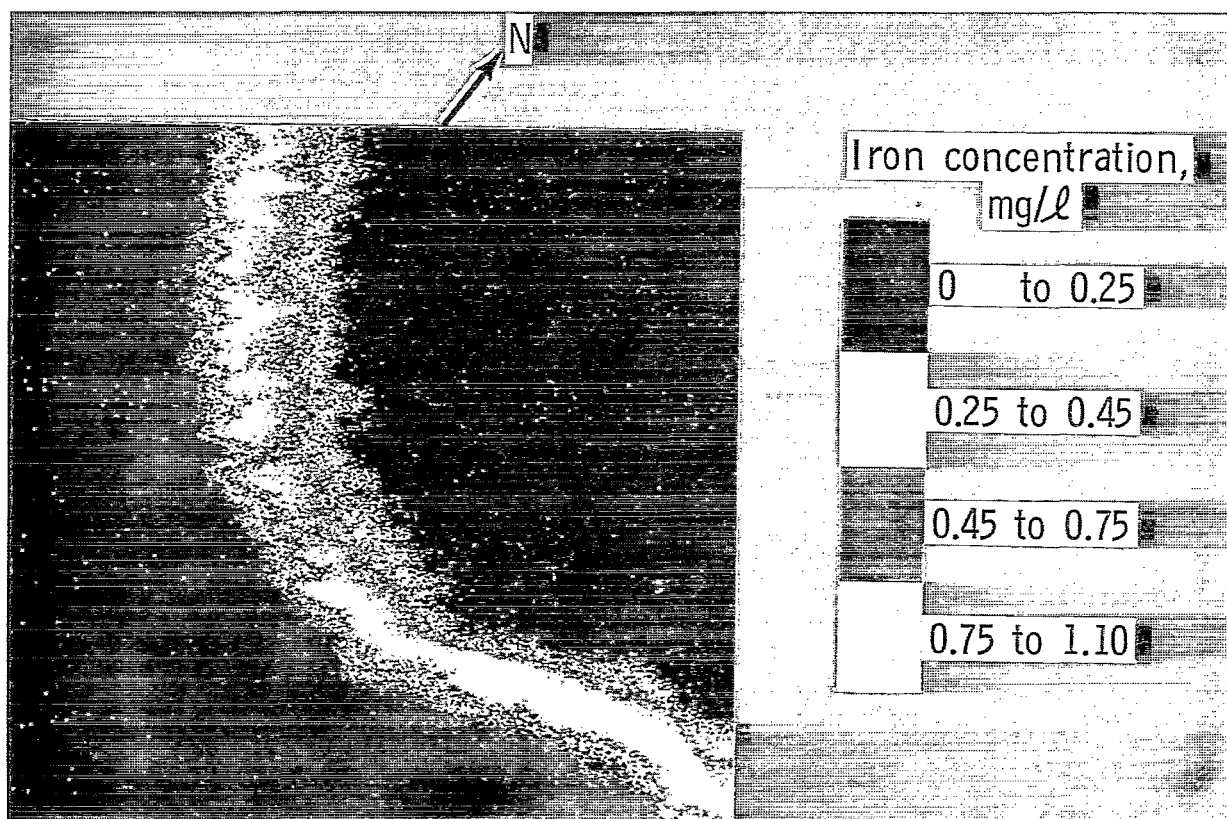


Figure 5.- Measured iron concentration as function of radiance ratio of band 2 to band 4.



L-78-121

Figure 6.- Particulate iron quantification map from spectral data collected on flight line over station 1-2. (Data set consists of every line and every other column.)



L-78-122

Figure 7.- Particulate iron quantification map from spectral data collected on flight line over station 3-1. (Data set consists of every line and every column.)

1. Report No. NASA TP-1275		2. Government Accession No.		3. Recipient's Catalog No.	
4. Title and Subtitle QUANTITATIVE MAPPING BY REMOTE SENSING OF AN OCEAN ACID-WASTE DUMP				5. Report Date October 1978	
				6. Performing Organization Code	
7. Author(s) Craig W. Ohlhorst				8. Performing Organization Report No. L-11927	
				10. Work Unit No. 176-30-34-05	
9. Performing Organization Name and Address NASA Langley Research Center Hampton, VA 23665				11. Contract or Grant No.	
				13. Type of Report and Period Covered Technical Paper	
12. Sponsoring Agency Name and Address National Aeronautics and Space Administration Washington, DC 20546				14. Sponsoring Agency Code	
15. Supplementary Notes					
16. Abstract  Results from quantitative analysis show that airplane remotely sensed spectral data can be used to quantify and map an acid-waste dump in terms of its particulate iron concentration. These same data, however, could not be used to map the dump in terms of total suspended solids, organic suspended solids, or inorganic suspended solids concentrations. A single-variable equation using the ratio of band 2 (440 to 490 nm) radiance to band 4 (540 to 580 nm) radiance was used to quantify the iron concentration in the acid-waste dump. The acid waste that was mapped varied in age from freshly dumped to $3\frac{1}{2}$ hr. Particulate iron concentrations in the acid waste were estimated to range up to 1.1 mg/l at a depth of 0.46 m. A classification technique was developed to identify pixels in the data set affected by Sun glitter.					
17. Key Words (Suggested by Author(s))  Quantification      Acid waste Water pollution Remote sensing Ocean dumping Sun-glitter classification technique			18. Distribution Statement  Unclassified - Unlimited		
19. Security Classif. (of this report)  Unclassified			20. Security Classif. (of this page)  Unclassified		21. No. of Pages  25
					22. Price*  \$4.00
Subject Category 45					

\* For sale by the National Technical Information Service, Springfield, Virginia 22161

NASA-Langley, 1978

National Aeronautics and  
Space Administration

Washington, D.C.  
20546

Official Business

Penalty for Private Use, \$300

THIRD-CLASS BULK RATE

Postage and Fees Paid  
National Aeronautics and  
Space Administration  
NASA-451



4 1 1U,E, 092978 S00903DS  
DEPT OF THE AIR FORCE  
AF WEAPONS LABORATORY  
ATTN: TECHNICAL LIBRARY (SUL)  
KIRTLAND AFB NM 87117

**NASA**

---

POSTMASTER: If Undeliverable (Section 158  
Postal Manual) Do Not Return